ISIJ International, Vol. 54 (2014), No. 2, pp. 437–444

Review

Phase-field Modeling and Simulations of Dendrite Growth

Tomohiro TAKAKI*

Mechanical and System Engineering, Kyoto Institute of Technology, Matsugasaki, Sakyo, Kyoto, 606-8585 Japan.

(*Received on October 1, 2013; accepted on November 15, 2013*)

The phase-field method has recently emerged as the most powerful computational tool for simulating complicated dendrite growth. However, these simulations are still limited to two-dimensional or small three-dimensional spaces; therefore, to realistic and practical dendritic structures, it is crucial to develop a large-scale phase-field simulation technique. This review discusses the phase-field modeling and simulations of dendrite growth from the fundamental model to cutting-edge very-large-scale simulations. First, phase-field models for the dendrite growth of pure materials and binary alloys and their histories are summarized. Then, models and studies of interface anisotropy, polycrystalline solidification, and solidification with convection, which are very important in dendritic solidification, are reviewed. Finally, by introducing very-large-scale phase-field simulations performed recently using a graphics processing unit supercomputer, the power, potential and importance of the very-large-scale phase-field simulation are emphasized.

KEY WORDS: phase-field method; solidification; dendrite; high-performance computing.

1. Introduction

Casting is performed at the beginning of all working processes. Although the solidification defects and microstructures formed during casting are reduced and changed in subsequent working processes such as hot-rolling, cold-rolling, and heat treatment, the solidification defects are not eliminated perfectly, and the solidification microstructures still strongly affect the microstructure evolution in the following working processes. Therefore, in order to improve the properties of the final product and to reduce the cost of the following working processes, it is very important to accurately control the solidification microstructures. Many solidification microstructures are formed through the growth of dendrites, which are typical structures grown during solidification.[1–3] Therefore, in order to accurately control the solidification microstructures, it is crucial to control and predict dendrite growth. Recent advances in in situ techniques for the observation of metallic material solidification by synchrotron X-ray imaging[4–14] have been improving our understanding of dendritic growth. However, in the present situation, those in situ observations are limited to thin samples that are essentially two-dimensional (2D) or small systems in which only a small number of dendrites grow, whereas the collective behavior of many dendrites in three-dimensional (3D) space is of primary importance in controlling the solidification microstructures. Therefore, to gain further understanding of dendrite growth, we need numerical simulation techniques for modeling dendrite growth in addition to further progress in experimental techniques.

Although many numerical techniques for simulating dendrite growth have been investigated, it has been difficult to reproduce the complicated dendrite morphology and its spatio-temporal evolution, which is governed by thermal and solutal fields. In this context, the success of the dendritic growth simulation by Kobayashi[15] brought the phase-field method into the spotlight. The phase-field method can avoid the difficulties in solving the free-boundary problem by alternatively solving the time evolution equation of the phase-field variable ϕ, which was newly introduced to express phase state of the material (solid or liquid). In this approach, the sharp interface is replaced by a diffuse interface with a finite thickness, where the phase-field variable ϕ changes smoothly and steeply, for example from $\phi = 0$ in liquid to $\phi = 1$ in solid. This idea enabled us to simulate the interface migration without tracking the interface. For this reason, the phase-field method can be considered an ambiguous or vague method; however, because it is very versatile, it is used as a powerful numerical tool for simulating not only dendrite growth but also various material microstructures. **Figure 1** shows the changes in the number of pub-

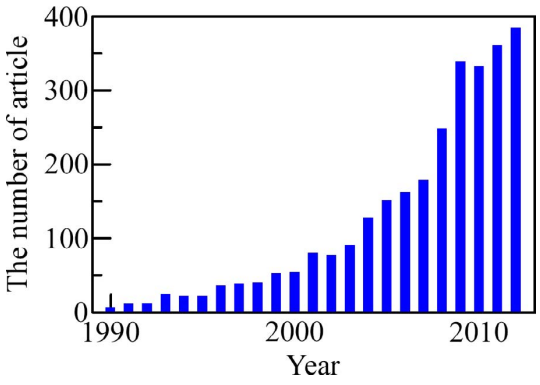

Fig. 1. Changes in number of papers published with "phase field" in title or key words from 1990 to 2012 according to SCOPUS database. (Online version in color.)

* Corresponding author: E-mail: takaki@kit.ac.jp
DOI: http://dx.doi.org/10.2355/isijinternational.54.437

lished articles whose title or key words include the phrase "phase field" according to the SCOPUS database. As can be seen in the figure, the number of articles regarding the phase-field method exponentially increases from 1990 after Kobayashi's successful dendrite growth phase-field simulation. Today, phase-field models for various problems have been developed, and the method has attained maturity. On the other hand, phase-field computations need fine numerical lattices to express smooth changes in the phase-field variable in small interfaces. Hence, the present dendrite growth computations are limited to 2D or to 3D with a small number of dendrites. As a next stage in phase-field research, development of large-scale simulation techniques is a key to reproducing realistic and practical material microstructure formation. **Figure 2** shows a large-scale phase-field simulation of directional solidification of a binary alloy, which was performed using the graphics processing unit (GPU) supercomputer TSUBAME2.0 at Tokyo Institute of Technology, Japan. The ACM Gordon Bell Award Special Achievement in Scalability and Time-to-Solution was awarded for this achievement in 2011.[16] We believe that this advance represents a great opportunity for phase-field study and marks the beginning of very-large-scale phase-field simulations.

This review summarizes the modeling and history of the phase-field method for dendrite growth simulation and introduces very-large-scale dendrite growth simulations employing the phase-field method that we performed recently.[17] Because there are many excellent and detailed review papers on phase-field methods for the simulation of dendrite solidification[18–26] or various other material microstructures,[27–35] this review is an attempt to cover, in a simple form, approaches ranging from the fundamental to the cutting edge of phase-field modeling, as well as simulations for beginners in the phase-field method and younger researchers.

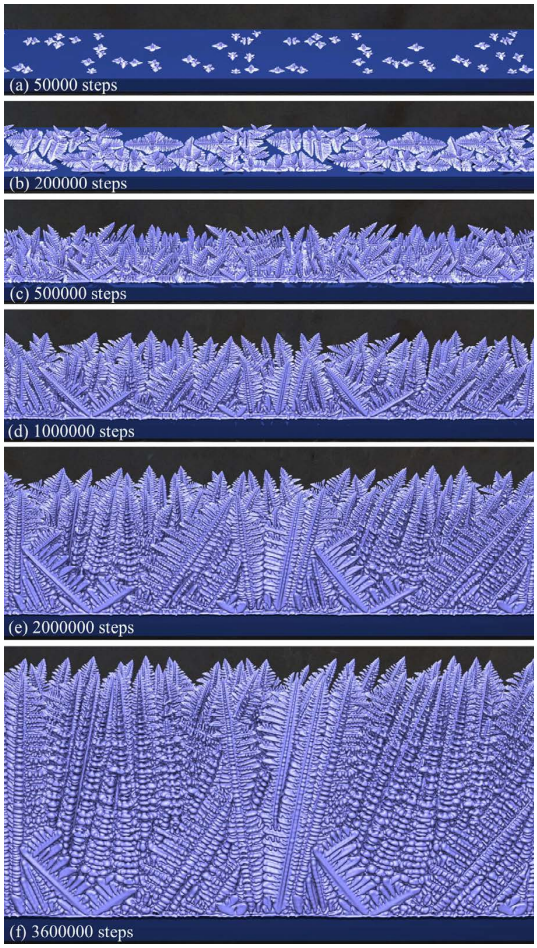

Fig. 2. Time slices showing competitive dendritic growth during directional solidification of Al–Si alloy. This phase-field simulation was performed in a computational domain of 3.072 mm × 0.768 mm × 3.072 mm (4 096 × 1 024 × 4 096 lattices) using GPU supercomputer TSUBAME2.0 at Tokyo Institute of Technology. (Online version in color.)

2. Phase-field Modeling and Its History for Dendrite Growth Simulation

In this chapter, first, the simple phase-field model that is the basis of all more complicated phase-field models is briefly explained. Next, phase-field models of dendritic growth for pure materials and binary alloys are summarized, with a short history. Then, the interface anisotropy, which is very important to the formation of the dendrite morphology, polycrystalline solidification simulations, and simulations of solidification with convection are reviewed, in this order.

2.1. Fundamental Phase-field Model

In the derivation of the phase-field equations, we first define the phase-field variable ϕ. Here, let us define $\phi = 0$ in liquid and $\phi = 1$ in solid. Then, by using the phase-field variable ϕ, we construct a free energy functional F. Considering a solid-liquid coexistence system with bulk free energies and interface energy, the simplest free energy functional F can be written as follows:

$$F = \int_V f dV \quad , \quad \text{..... (1)}$$

where the free energy density f can be expressed as

$$f = f_{chem} + f_{doub} + f_{grad} \quad , \quad \text{..... (2)}$$

with

$$f_{chem} = p(\phi) f_S + \left(1 - p(\phi)\right) f_L \quad , \quad \text{..... (3)}$$

$$f_{doub} = W q(\phi) \quad , \quad \text{..... (4)}$$

$$f_{grad} = \frac{a^2}{2} |\nabla \phi|^2 \quad . \quad \text{..... (5)}$$

Here, f_{chem} is the chemical free energy density, which is expressed by interpolating the bulk free energies in the solid f_S and liquid f_L with a monotonically increasing function $p(\phi)$. For $p(\phi)$, $p(\phi) = \phi^3(10 - 15\phi + 6\phi^2)$ or $p(\phi) = \phi^2(3 - 2\phi)$ is often used. The f_{doub} component is the double-well potential, which represents the energy barrier at the solid-liquid interface, where W is the height of the energy barrier and $q(\phi)$ is a double-well function, for which $q(\phi) = \phi^2(1 - \phi)^2$ is often used. Finally, f_{grad} is the gradient energy density with gradient coefficient a. In Eq. (3), f_{chem} is the bulk energy and $f_{doub} + f_{grad}$ corresponds to the interface energy.

Next, we derive the time evolution equation of ϕ by following the second law of thermodynamics. Because the phase-field variable ϕ is a nonconserved value, we use the Allen-Cahn equation or time-dependent Ginzburg-Landau equation,

$$\frac{\partial \phi}{\partial t} = -M_\phi \frac{\delta F}{\delta \phi} \quad , \quad \text{..... (6)}$$

where the functional derivative $\delta F/\delta\phi$ can be calculated as

$$\frac{\delta F}{\delta\phi}=\frac{\partial f_{chem}}{\partial\phi}+\frac{\partial f_{doub}}{\partial\phi}-\nabla\cdot\frac{\partial f_{grad}}{\partial(\nabla\phi)}$$
$$=30\phi^2(1-\phi)^2(f_S-f_L)+2W\phi(1-\phi)(1-2\phi)-a^2\nabla^2\phi. \quad \text{..... (7)}$$

Here, we used $p(\phi) = \phi^3(10 - 15\phi + 6\phi^2)$. Substituting Eq. (7) into Eq. (6), we obtain the time evolution equation of the phase-field variable ϕ

$$\frac{\partial\phi}{\partial t}=M_\phi\left[a^2\nabla^2\phi+4W\phi(1-\phi)\left(\phi-\frac{1}{2}+\frac{15}{2W}\phi(1-\phi)(f_L-f_S)\right)\right]. \quad \text{..... (8)}$$

As can be seen from Eq. (8), the phase-field equation reduces to a reaction-diffusion equation, where first and second terms in the bracket on the right-hand side are the diffusion and reaction terms, respectively. Equation (8) expresses the interface migration as a balance between smoothing by the diffusion term and steepening by the reaction term.

The coefficients a, W, and M_ϕ in Eq. (8) are related to the interface thickness δ, interface energy γ, and interface mobility M as follows:

$$a=\sqrt{\frac{3\delta\gamma}{b}}\ , \quad \text{..... (9)}$$

$$W=\frac{6\gamma b}{\delta}\ , \quad \text{..... (10)}$$

$$M_\phi=\frac{\sqrt{2W}}{6a}M\ , \quad \text{..... (11)}$$

where, $b = 2\tanh^{-1}(1 - 2\phi_0)$. Setting $\phi_0 = 0.1$, we obtain $b = 2.2$. By solving Eq. (8) under the one-dimensional (1D) equilibrium condition $\partial\phi/\partial t = 0$, we can derive the 1D equilibrium profile of ϕ as

$$\phi_{eq}=\frac{1}{2}\left\{1-\tanh\frac{\sqrt{2W}}{2a}x\right\}. \quad \text{..... (12)}$$

Figure 3 shows the relations among ϕ_{eq}, ϕ_0, and δ. Equations (9) and (10) can be derived from the relations $\delta = x_1 - x_2$ and $\gamma=\int_{-\infty}^{+\infty}\left(f_{doub}+f_{grad}\right)dx$. Equation (11) can be derived by comparing the 1D steady growth condition of Eq. (8) to a constant velocity $V = M(f_L - f_S)$.

To determine f_S and f_L in Eq. (8), which are functions of temperature and/or concentration, the thermal conduction equation and/or diffusion equation are solved at the same time. Then, because the distributions of temperature and concentration in the interface region change depending on the interface thickness, the interface migration rate also changes depending on the interface thickness. Therefore, the results are usually not quantitative. On the other hand, if $f_S - f_L$ is a constant, Eq. (8) provides quantitative results independent of the interface thickness. Now, setting $\beta=\frac{15}{2W}\phi(1-\phi)(f_L-f_S)$, simulation should be performed in the range of $-0.5 \le \beta \le 0.5$. Then, because $\beta \propto \delta(f_L - f_S)$, we need a small interface thickness δ when $f_L - f_S$ is large, and we can use a large δ when $f_L - f_S$ is small. This is a very important point when choosing the value of δ or the size of the numerical lattice Δx. We usually use $\delta = 4\Delta x \sim 8\Delta x$, depending on the problem. In addition, an interface thickness satisfying $\Delta x \le R/5$ should be used, where R is the dendrite tip radius.

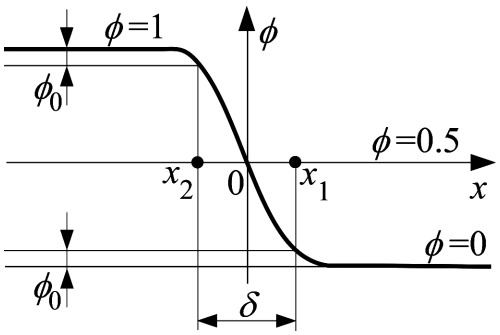

Fig. 3. Relation between equilibrium profile of phase-field ϕ_{eq} and interface thickness δ.

2.2. Pure Material Solidification

In a phase-field simulation of the dendrite growth of a pure material, a thermal conductivity equation describing the latent heat release from solid-liquid interface, such as

$$\frac{\partial T}{\partial t}=\kappa\nabla^2T+\frac{L}{c_p}\frac{\partial p(\phi)}{\partial t}\ , \quad \text{..... (13)}$$

is solved in addition to Eq. (8). Here, T is temperature, κ is the thermal diffusion coefficient, L is latent heat, and c_p is specific heat. In pure material solidification, a thermodynamic driving force $f_L - f_S = L(T_m - T)/T_m$ is usually used in Eq. (8), where T_m is the melting temperature.

Although some studies on phase-field models for the solidification of pure material were performed before 1990,[36–39] actual dendrite growth simulation using the phase-field method was first achieved by Kobayashi[15] by introducing the interface anisotropy (see Section 2.4), which is very important to the formation of four- or six-fold symmetry of the dendrite shape. Kobayashi's paper[15] was published in 1993, and it only discussed the simulation of 2D dendrites. However, he had already succeeded in simulating 3D dendrite growth and produced movies of it before 1990.[40] These results fascinated many related researchers. By imposing a sharp interface limit where the interface width goes to zero, the parameters in phase-field equation could be related to the material parameters such as the interface energy and kinetic coefficient, and detailed simulations using the material parameters were performed.[41,42] Because those models were derived from a free energy functional even though the temperature changes, a thermodynamically consistent model was also derived from the entropy functional.[43,44] It was pointed out that the results change depending on the interface thickness, because the temperature profile in the interface changes when the interface thickness changes. Therefore, the above models are valid only under the conditions of a small interface thickness and high undercooling.[45,46] Karma[46–49] solved this problem by imposing a thin interface limit on the phase-field equations, which enabled quantitative simulations independent of the interface thickness under the low-undercooling condition, where the kinetic undercooling is negligibly small compared to the curvature undercooling. In

other words, the phase-field mobility shown in Eq. (11) does not include the interface kinetic coefficient[50] Karma's quantitative model was derived for a pure material with equal thermal diffusivities in the solid and liquid phases, and it was also applied to different thermal diffusivities.[51]

2.3. Binary Alloy Solidification

A phase-field model for binary alloy solidification has also been developed, similarly to that for the pure material described in section 2.1. Wheeler, Boettinger, and McFadden (WBM) first developed a phase-field model for isothermal solidification of a binary alloy, which is called the WBM model,[52–54] by directly extending the pure material model[41,42] to a binary alloy. In order to use the WBM model under nonisothermal conditions, Warren and Boettinger[55] derived the phase-field equations for binary alloy solidification from the entropy functional.[43] With this model, realistic and beautiful 2D dendrite growth in a binary alloy was successfully simulated under both isothermal[55] and nonisothermal[56,57] conditions. However, because the solute concentration changes in the interface region, the results change depending on the interface thickness. Kim, Kim, and Suzuki (KKS) pointed out that in the free energy density defined in the WBM model, an extra energy term appears in the interface region.[58] Although the interfacial region was defined in the WBM model as a mixture of solid and liquid with the same composition and different chemical potentials, in the KKS model, the interfacial region was defined as a mixture of solid and liquid with different compositions, as $c = p(\phi)c_S + (1 - p(\phi))c_L$, and the same chemical potential, $\partial f_S/\partial c_S = \partial f_L/\partial c_L = \mu_c$. In this case, Eq. (8) can be modified as

$$\frac{\partial \phi}{\partial t} = M_\phi \left[a^2 \nabla^2 \phi + 4W\phi(1-\phi) \left(\phi - \frac{1}{2} + \frac{15}{2W}\phi(1-\phi)\left(f_L(c_L) - f_S(c_S) - (c_L - c_S)\mu_c \right) \right) \right]. \quad \text{..... (14)}$$

The diffusion equation can be derived from the Cahn-Hilliard equation

$$\frac{\partial c}{\partial t} = \nabla \cdot \left[M_\phi \left(\nabla \frac{\delta F}{\delta c} \right) \right], \quad \text{..... (15)}$$

as

$$\frac{\partial c}{\partial t} = \nabla \cdot (D \nabla c) + \nabla \cdot \left[D \frac{dp(\phi)}{d\phi}(c_L - c_S) \nabla \phi \right], \quad \text{... (16)}$$

where D is the diffusion coefficient. When KKS's idea is introduced, the extra energy caused by the interpolation of the bulk energies of the liquid and solid phases can be eliminated. However, the KKS model was inadequate to quantitatively model the low-growth-rate regime. To overcome this limitation, Karma has developed a quantitative phase-field model of dilute binary alloy solidification with zero diffusivity in the solid (one-side model) in such a low-growth-rate regime.[59] In Karma's quantitative model, an antitrapping current term that controls solute diffusion across the interface is added to the diffusion equation. The model was also successfully applied to nonisothermal solidification.[60] Recently, Ohno and Matsuura developed a quantitative phase-field model for dilute alloy solidification with arbitrary value of the solid diffusivity.[61,62] The solute diffusivity in a solid is very important in the solidification of steel, which is the most important material for practical applications. Although these quantitative models introducing an antitrapping current term are common at present, these models are not universal and are only valid for slow solidification. Therefore, the development of a phase-field model that enables the simulation of binary alloy solidification under all thermal conditions is being researched even today.[63]

2.4. Interface Anisotropy

The morphology of growing dendrites depends sensitively on the anisotropy of the interface energy and interface kinetics, even though the anisotropy is small, ~ 1%, especially for the interface energy.[3,20,26] In many cases, the anisotropy of the interface energy is included in the gradient coefficient as

$$a(\nabla\phi) = \bar{a}(1-3\zeta)\left\{ 1 + \frac{4\zeta}{1-3\zeta} \frac{\left(\frac{\partial\phi}{\partial x}\right)^4 + \left(\frac{\partial\phi}{\partial y}\right)^4 + \left(\frac{\partial\phi}{\partial z}\right)^4}{|\nabla\phi|^4} \right\}, \quad \text{..... (17)}$$

for a 3D cubic structure. Here, ζ is the strength of the anisotropy and $\bar{a}$ is the average value of a. In 2D, Eq. (17) reduces to

$$a(\nabla\phi) = \bar{a}(1-3\zeta)\left\{ 1 + \frac{4\zeta}{1-3\zeta} \frac{\left(\frac{\partial\phi}{\partial x}\right)^4 + \left(\frac{\partial\phi}{\partial y}\right)^4}{|\nabla\phi|^4} \right\} = \bar{a}\left[1 + \zeta\cos(4\Theta) \right], \quad \text{..... (18)}$$

where Θ is the angle between the x-axis and the interface normal. Using Eq. (17) in 3D, Eq. (8) can be modified as

$$\frac{\partial\phi}{\partial t} = M_\phi \left[\nabla \cdot \left(a^2 \nabla\phi \right) + \frac{\partial}{\partial x}\left\{ a \frac{\partial a}{\partial\left(\frac{\partial\phi}{\partial x}\right)} (\nabla\phi)^2 \right\} + \frac{\partial}{\partial y}\left\{ a \frac{\partial a}{\partial\left(\frac{\partial\phi}{\partial y}\right)} (\nabla\phi)^2 \right\} + \frac{\partial}{\partial z}\left\{ a \frac{\partial a}{\partial\left(\frac{\partial\phi}{\partial z}\right)} (\nabla\phi)^2 \right\} + 4W\phi(1-\phi)\left(\varphi - \frac{1}{2} + \frac{15}{2W}\phi(1-\phi)(f_L - f_S) \right) \right]. \quad \text{..... (19)}$$

Experimental measurements of the anisotropy of the interface energy are limited to those by Napolitano *et al.*[64–66] and the anisotropy of the interface kinetics has not been reported. Therefore, at present, atomic-scale simulations such as molecular dynamics (MD) simulations are believed to be the most powerful tool for evaluating this anisotropy. Hoyt *et al.*[67] have developed a method to compute such a small anisotropy of the solid-liquid interface energy, and the anisotropies of the interface energies for various systems

have been simulated by their group[68–74] and others.[75–84] Many MD simulations computing the solid-liquid interface kinetics have been performed.[85–92] Phase-field dendritic growth simulations using the interface anisotropy calculated by these MD simulations have also been performed successfully.[93–95] This coupled computation is believed to be a promising technique for accurate dendrite growth simulation.

For a high-interface-anisotropy problem, a special treatment is needed for the anisotropy function. In 2D facet[96–99] or needle[100,101] crystal growth simulations, a convexification scheme proposed by Eggleston *et al.*[102] has been widely used. However, it was pointed out that this scheme cannot express the nucleation of facets. Therefore, various generalization schemes for high anisotropy have been developed.[103–107] A cusp interface energy model[108,109] has also been used to treat the facet and a high-anisotropy kinetic coefficient[110,111] has been modeled. Recently, dendrite growth simulations have been performed both in the 2D[112–114] and 3D[115,116] spaces for materials with the hexagonal close-packed structure, such as Mg alloys, which are the lightest metallic materials, and therefore, very important as future industrial materials.

2.5. Polycrystalline Solidification

To simulate polycrystalline solidification in which multiple dendrites grow in different directions, there are roughly two types of phase-field models. One is a multi-phase-field (MPF) model[117–129] that uses multiple phase-field variables to distinguish different grains and/or phases, and the other is a KWC[130–135] (Kobayashi, Warren and Carter)[130]-type model, where two order parameters representing the phase-field and orientation-field are used. The MPF model is a general model for simulating the solidification of multiple-phase and multiple-component alloys, and it can treat solidification and grain growth simultaneously. Among the various models of this type, the MPF model developed by Steinbach *et al.*[119] is used most widely. In the MPF model, a double-obstacle function instead of a double-well function is used to make the energy at the triple point larger than that in the interface. KWC-type models are useful for simulating the growth of multiple dendrites until they impinge. However, it is difficult to model the grain growth quantitatively. Nevertheless, KWC-type models are very interesting, and Gránásy *et al.* successfully simulated polycrystalline solidification and spherulite growth using their own KWC-type model.[21,32,100,101,136,137]

2.6. Solidification with Convection

Convection plays dominant role in the formation of the solidification microstructure in real situations,[26] although almost all dendrite growth simulations are performed under conditions without convection. In fluid dynamics, the diffuse interface model has been used for the two-phase flow problem, among others, for a long time.[138] By applying such know-how in fluid dynamics to solidification, Anderson *et al.*,[139–141] Tönhardt *et al.*,[142–144] and Beckermann *et al.*[145–148] developed models for solidification with convection by coupling the phase-field equations and Navier-Stokes equations. Beckermann *et al.*[145–148] introduced a friction term into the Navier-Stokes equations to impose a no-slip condition at the solid-liquid interface, which acts as a distributed momentum sink in the interface region where the phase-field changes. Since then, many phase-field simulations of dendritic growth with forced flows and natural convection have been performed. Because these simulations have high computational costs, adaptive mesh (ADM) techniques,[149–151] the numerically efficient Lattice Boltzmann method,[152–157] and parallel computing[158,159] have been used. However, for the dendrite growth problem with convection, 2D simulations[160–165] provide results completely different from the real 3D phenomena. Therefore, recently, 3D simulations[157,166–170] have been performed, although they are limited to small regions with small numbers of dendrites.

3. Large-scale Dendrite Growth Simulations

The major disadvantage of the phase-field method is that many numerical lattices are required to achieve a smooth distribution of the phase-field in the small interface region. Therefore, the dendrite growth simulations performed so far have been limited to 2D or to 3D with a small computational region. To overcome this disadvantage, ADM techniques have been widely used in 2D[142,144,150,171–178] and 3D[169,170,179–183] dendrite growth simulations. Because the regions in which the phase-field variable changes are limited to near the interface region, the ADM can drastically reduce the number of numerical lattices, which makes it promising for simultaneous application with quantitative phase-field models. Parallel computations[125,184–186] have also been applied to large-scale phase-field simulations. Nevertheless, the 3D dendrite growth simulations reported so far have been restricted to one or a small number of dendrites,[186,187] a small region only around the tip,[188] narrow channels,[189] or cellular structures,[81,190–192] even though interactions between multiple dendrites are very important in real solidification microstructures. Hence, in the next step of phase-field study, it is crucial to develop large-scale simulation technologies.

Recently, numerical computations using GPUs, which were originally developed as visualization processing units, have become attractive in high-performance computing as an alternative to CPU (central processing unit)-based parallel computing. High performance is possible because each GPU has many cores, from several hundred to thousands, in contrast to the CPU, which has only a few cores. Therefore, GPU computation is well suited for stencil computation. Recently, we have shown that phase-field dendrite growth simulations can be greatly accelerated by GPUs,[193] which enabled the first-ever petascale phase-field dendrite growth computation with single precision.[16] This was realized by using 4 000 GPUs along with 16 000 CPUs of the TSUBAME 2.0 supercomputer at Tokyo Institute of Technology. The high performance was achieved by building our simulation code from scratch in the GPU-specific language CUDA and introducing an overlapping technique that avoids performance degradation due to inter-GPU communication.[16]

Figure 2 shows the competitive growth processes of multiple dendrites during directional solidification of a Al–Si binary alloy. This simulation was carried out in a system with dimensions of 3.072 mm × 0.768 mm × 3.072 mm (4 096 × 1 024 × 4 096 lattices) in four million computational steps. The number of GPUs used in this simulation was 512, and the computational time was about 110 hours. In Fig. 2, we can observe a series of realistic directional solid-

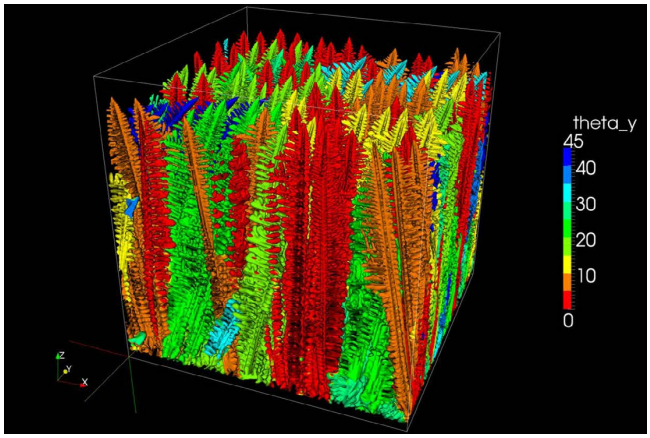

Fig. 4. Dendrite morphology at 360 million steps in very-large-scale phase-field simulation using a computational domain of 3.072 mm × 3.078 mm × 3.072 mm (4 096 × 4 104 × 4 096 lattices). (Online version in color.)

ification processes from nucleation to competitive growth in 3D. First, 32 solid seeds initially nucleated at the bottom wall grow into star shapes (a) and then cover the bottom surface through lateral growth (b). After that, the dendrites begin growing in preferred growth directions close to the heat flow direction (c). As the solidification front proceeds upward, the number of dendrites gradually decreases because of competitive growth of the dendrites (d)–(f). Furthermore, very recently, we performed a much larger computation in a system with dimensions of 3.072 mm × 3.078 mm × 3.072 mm (4 096 × 4 104 × 4 096 lattices) using 768 GPUs.[17] **Figure 4** shows the dendrite morphologies at 360 million steps, where the color indicates the inclination angle of the dendrites relative to the bottom surface. Almost all the conditions are same as those in Fig. 2, except for the boundary conditions in the thickness direction, computational domain size, and the number of initial solid seeds (128). This 3D, very-large-scale simulation has enabled us to see the effect of the preferred growth direction on the dendrite selection phenomena in detail, as well as the detailed interactions among neighboring dendrites.[17] From this simulation, it was concluded that a relatively large number of dendrites with large inclination angles can survive and that the dendrite interactions during competitive growth are very complicated. We can also remove each dendrite grown from the same seed. **Figure 5** shows four representative dendrites among the 46 dendrites that survived at the time shown in Fig. 4. **Table 1** shows the number of dendrites categorized by inclination angle θ and with and without branches. Dendrites without branches are further categorized into single or multiple dendrites. The four dendrites shown in Fig. 5 are indicated in Table 1. It is observed that it is relatively difficult for branching to occur for a dendrite with a small θ. On the other hand, branching is necessary for a highly inclined dendrite to grow continuously.

As shown above, we can obtain much information from 3D large-scale simulations of multiple dendrites. Lately, comparisons of phase-field computations and in situ observations have been reported.[194–200] This is a very important development in material science. However, the phase-field computations performed in those reports are limited to 2D or small 3D spacings, which are not consistent with the actual experimental conditions. From these points of view, we still need to develop large-scale phase-field simulation techniques.

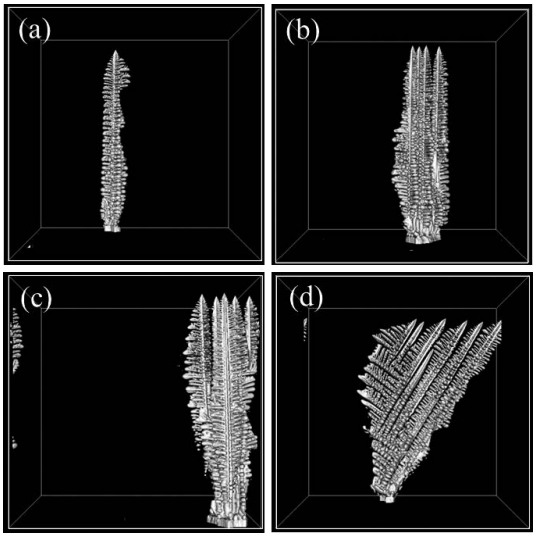

Fig. 5. Number of dendrites categorized by inclination angle θ with and without branches among 46 dendrites that survived in Fig. 4.

Table 1. Number of dendrites categorized by inclination angle with and without branches.

	no-branching		branching
θ[°]	single	multiple	
0–10	11 [Fig. 5(a)]	4 [Fig. 5(b)]	8 [Fig. 5(c)]
10–20	4	3	8
20–30	1	0	5
30–45	0	0	2 [Fig. 5(d)]

4. Conclusions

Today, more than twenty years since Kobayashi successfully simulated dendrite growth using the phase-field method, the number of articles regarding this method has rapidly increased, and it has emerged as a powerful numerical tool for simulating the microstructure evolution of various materials. In dendrite growth simulations, quantitative models for pure materials, binary alloys, and multiple-component alloys have been developed, and polycrystalline solidification and dendrite growth with convection have been simulated. In addition, progress in in situ observation technology has made direct comparison of simulations and experiments possible. For further progress in solidification science, the development of very-large-scale phase-field simulation technology is indispensable. We believe our recent computations using a GPU supercomputer will open the road to such very-large-scale phase-field simulations.

Acknowledgements

The author would like to thank Professor Munekazu Ohno at Hokkaido University for providing valuable comments about quantitative phase-field model. Thanks are also given to Professor Takayuki Aoki and Professor Takashi Shimokawabe at Tokyo Institute of Technology and Akinori

Yamanaka at Tokyo University of Agriculture and Technology for providing fruitful advice about GPU computation. This work was supported by JSPS KAKENHI Grant Number 25289006.

REFERENCES

1) J. S. Langer: *Rev. Mod. Phys.*, **52** (1980), 1.
2) S. A. David and T. DebRoy: *Science*, **257** (1992), 497.
3) W. J. Boettinger, S. R. Coriell, A. L. Greer, A. Karma, W. Kurz, M. Rappaz and R. Trivedi: *Acta Mater.*, **48** (2000), 43.
4) R. H. Mathiesen, L. Arnberg, F. Mo, T. Weitkamp and A. Snigirev: *Phys. Rev. Lett.*, **83** (1999), 5062.
5) R. H. Mathiesen, L. Arnberg, K. Ramsøskar, T. Weitkamp, C. Rau and A. Snigirev: *Metall. Mater. Trans. B*, **33** (2002), 613.
6) H. Yasuda, I. Ohnaka, K. Kawasaki, A. Sugiyama, T. Ohmichi, J. Iwane and K. Umetani: *J. Cryst. Growth*, **262** (2004), 645.
7) T. Schenk, H. N. Thi, J. Gastaldi, G. Reinhart, V. Cristiglio, N. Mangelinck-Noël, H. Klein, J. Härtwig, B. Grushko, B. Billia and J. Baruchel: *J. Cryst. Growth*, **275** (2005), 201.
8) G. Reinhart, A. Buffet, H. Nguyen-Thi, B. Billia, H. Jung, N. Mangelinck-Noël, N. Bergeon, T. Schenk, J. Härtwig and J. Baruchel: *Metall. Mater. Trans. A*, **39A** (2008), 865.
9) H. Yasuda, Y. Yamamoto, N. Nakatsuka, M. Yoshiya, T. Nagira, A. Sugiyama, I. Ohnaka, K. Uesugi and K. Umetani: *Int. J. Cast Metal. Res.*, **22** (2009), 15.
10) S. Terzi, L. Salvo, M. Suery, A. K. Dahle and E. Boller: *Acta Mater.*, **58** (2010), 20.
11) H. Yasuda, T. Nagira, M. Yoshiya, N. Nakatsuka, A. Sugiyama, K. Uesugi and K. Umetani: *ISIJ Int.*, **51** (2011), 402.
12) H. Nguyen-Thi, L. Salvo, R. H. Mathiesen, L. Arnberg, B. Billia, M. Suery and G. Reinhart: *Comptes Rendus Physique*, **13** (2012), 237.
13) D. Tolnai, P. Townsend, G. Requena, L. Salvo, J. Lendvai and H. P. Degischer: *Acta Mater.*, **60** (2012), 2568.
14) J. Baruchel, M. Di Michiel, T. Lafford, P. Lhuissier, J. Meyssonnier, H. Nguyen-Thi, A. Philip, P. Pernot, L. Salvo and M. Scheel: *Comptes Rendus Physique*, **14** (2013), 208.
15) R. Kobayashi: *Physica D*, **63**(1993), 410.
16) T. Shimokawabe, T. Aoki, T. Takaki, A. Yamanaka, A. Nukada, T. Endo, N. Maruyama and S. Matsuoka: Proc. of SC11, ACM, New York, (2011), 1.
17) T. Takaki, T. Shimokawabe, M. Ohno, A. Yamanaka and T. Aoki: *J. Cryst. Growth*, **382** (2013), 21.
18) A. A. Wheeler, N. A. Ahmad, W. J. Boettinger, R. J. Braun, G. B. McFadden and B. T. Murray: *Adv. Space Res.*, **16** (1995), 163.
19) W. J. Boettinger, J. A. Warren, C. Beckermann and A. Karma: *Annu. Rev. Mater. Sci.*, **32** (2002), 163.
20) J. Hoyt: *Mater. Sci. Eng.: R: R*, **41** (2003), 121.
21) U. Hecht, L. Gránásy, T. Pusztai, B. Böttger, M. Apel, V. Witusiewicz, L. Ratke, J. De Wilde, L. Froyen, D. Camel, B. Drevet, G. Faivre, S. G. Fries, B. Legendre and S. Rex: *Mater. Sci. Eng. R: Rep.*, **46** (2004), 1.
22) K. Nakajima, H. Zhang, K. Oikawa, M. Ohno and P. G. Jönsson: *ISIJ Int.*, **50** (2010), 1724.
23) B. Nestler and A. Choudhury: *Curr. Opin. Solid State Mater. Sci.*, **15** (2011), 93.
24) I. Steinbach: *JOM*, **65** (2013), 1096.
25) M. Ode, K. Seong Gyoon and T. Suzuki: *ISIJ Int.*, **41** (2001), 1076.
26) M. Asta, C. Beckermann, A. Karma, W. Kurz, R. Napolitano, M. Plapp, G. Purdy, M. Rappaz and R. Trivedi: *Acta Mater.*, **57** (2009), 941.
27) I. Steinbach: *Annu. Rev. Mater. Res.*, **43** (2013), 89.
28) I. Singer-Loginova and H. M. Singer: *Rep. Prog. Phys.*, **71** (2008), 106501.
29) H. Emmerich, H. Löwen, R. Wittkowski, T. Gruhn, G. I. Tóth, G. Tegze and L. Gránásy: *Adv. Phys.*, **61** (2012), 665.
30) N. Moelans, B. Blanpain and P. Wollants: *Calphad*, **32** (2008), 268.
31) T. Kitashima: *Philos. Mag.*, **88** (2008), 1615.
32) L. Gránásy, T. Pusztai, T. Börzsönyi, G. Tóth, G. Tegze, J. A. Warren and J. F. Douglas: *J. Mater. Res.*, **21** (2006), 309.
33) L. Q. Chen: *Annu. Rev. Mater. Sci.*, **32** (2002), 113.
34) I. Steinbach: *Modell. Simul. Mater. Sci. Eng.*, **17** (2009), 073001.
35) Y. Wang and J. Li: *Acta Mater.*, **58** (2010), 1212.
36) G. Caginalp: *Arch. Ration. Mech. An.*, **92** (1986), 205.
37) G. Caginalp: *Phys. Rev. A*, **39** (1989), 5887.
38) G. Caginalp and P. Fife: *Phys. Rev. B*, **33** (1986), 7792.
39) J. B. Collins and H. Levine: *Phys. Rev. B*, **31** (1985), 6119.
40) R. Kobayashi: *Exp. Math.*, **3** (1994), 59.
41) A. A. Wheeler, B. T. Murray and R. J. Schaefer: *Physica D: Nonlinear Phenomena*, **66** (1993), 243.
42) B. T. Murray, A. A. Wheeler and M. E. Glicksman: *J. Cryst. Growth*, **154** (1995), 386.
43) S. L. Wang, R. F. Sekerka, A. A. Wheeler, B. T. Murray, S. R. Coriell, R. J. Braun and G. B. McFadden: *Physica D: Nonlinear Phenomena*, **69** (1993), 189.
44) O. Penrose and P. C. Fife: *Physica D: Nonlinear Phenomena*, **43** (1990), 44.
45) S.-L. Wang and R. Sekerka: *Phys. Rev. E*, **53** (1996), 3760.
46) A. Karma and W.-J. Rappel: *Phys. Rev. E*, **53** (1996), R3017.
47) A. Karma and W.-J. Rappel: *Phys. Rev. Lett.*, **77** (1996), 4050.
48) A. Karma and W.-J. Rappel: *J. Cryst. Growth*, **174** (1997), 54.
49) A. Karma and W.-J. Rappel: *Phys. Rev. E*, **57** (1998), 4323.
50) T. Takaki and H. Kashima: *J. Cryst. Growth*, **337** (2011), 97.
51) R. F. Almgren: *SIAM J. App. Math.*, **59** (1999), 2086.
52) A. A. Wheeler, W. J. Boettinger and G. B. McFadden: *Phys. Rev. A*, **45** (1992), 7424.
53) A. A. Wheeler, W. J. Boettinger and G. B. McFadden: *Phys. Rev. E*, **47** (1993), 1893.
54) W. J. Boettinger, A. A. Wheeler, B. T. Murray and G. B. McFadden: *Mater. Sci. Eng. A*, **178** (1994), 217.
55) J. A. Warren and W. J. Boettinger: *Acta Metall.*, **43** (1995), 689.
56) W. J. Boettinger and J. A. Warren: *Metall. Mater. Trans. A*, **27** (1996), 657.
57) I. Loginova, G. Amberg and J. Ågren: *Acta Mater.*, **49** (2001), 573.
58) S. G. Kim, W. T. Kim and T. Suzuki: *Phys. Rev. E*, **60** (1999), 7186.
59) A. Karma: *Phys. Rev. Lett.*, **87** (2001), 115701.
60) J. C. Ramirez, C. Beckermann, A. Karma and H. J. Diepers: *Phys. Rev. E*, **69** (2004), 051607.
61) M. Ohno and K. Matsuura: *Phys. Rev. E*, **79** (2009), 031603.
62) M. Ohno: *Phys. Rev. E*, **86** (2012), 051603.
63) I. Steinbach, L. Zhang and M. Plapp: *Acta Mater.*, **60** (2012), 2689.
64) S. Liu, R .E. Napolitano and R. Trivedi: *Acta Mater.*, **49** (2001), 4271.
65) R. Napolitano and S. Liu: *Phys. Rev. B*, **70** (2004), 214103.
66) R. E. Napolitano, S. Liu and R. Trivedi: *Interface Sci.*, **10** (2002), 217.
67) J. Hoyt, M. Asta and A. Karma: *Phys. Rev. Lett.*, **86** (2001), 5530.
68) M. Asta, J. Hoyt and A. Karma: *Phys. Rev. B*, **66** (2002), 1001011.
69) D. Y. Sun, M. I. Mendelev, C. A. Becker, K. Kudin, T. Haxhimali, M. Asta, J. J. Hoyt, A. Karma and D. J. Srolovitz: *Phys. Rev. B*, **73** (2006), 024116.
70) C. Becker, D. Olmsted, M. Asta, J. Hoyt and S. Foiles: *Phys. Rev. Lett.*, **98** (2007), 125701.
71) A. A. Potter and J. J. Hoyt: *J. Cryst. Growth*, **327** (2011), 227.
72) J. Liu, R. L. Davidchack and H. B. Dong: *Comput. Mater. Sci.*, **74** (2013), 92.
73) D. Y. Sun, M. Asta and J. J. Hoyt: *Phys. Rev. B*, **69** (2004), 174103.
74) D. Y. Sun, M. Asta, J. J. Hoyt, M. I. Mendelev and D. J. Srolovitz: *Phys. Rev. B*, **69** (2004), 201021.
75) M. Amini and B. B. Laird: *Phys. Rev. B*, **78** (2008), 144112.
76) X. M. Bai and M. Li: *J. Chem. Phys.*, **124** (2006), 124707.
77) R. L. Davidchack and B. B. Laird: *Phys. Rev. Lett.*, **94** (2005), 086102.
78) R. L. Davidchack and B. B. Laird: *J. Chem. Phys.*, **118** (2003), 7651.
79) R. Hashimoto, Y. Shibuta and T. Suzuki: *ISIJ Int.*, **51** (2011), 1664.
80) B. B. Laird and R. L. Davidchack: *J. Phys. Chem. B*, **109** (2005), 17802.
81) F. Luo, X. R. Chen, L. C. Cai and G. F. Ji: *J. Chem. Eng. Data*, **55** (2010), 5149.
82) J. R. Morris: *Phys. Rev. B*, **66** (2002), 1441041.
83) J. R. Morris and X. Song: *J. Chem. Phys.*, **119** (2003), 3920.
84) H. Zhou, X. Lin, M. Wang and W. Huang: *J. Cryst. Growth*, **377** (2013), 107.
85) J. J. Hoyt, M. Asta and A. Karma: *Interface Sci.*, **10** (2002), 181.
86) M. Amini and B. Laird: *Phys. Rev. Lett.*, **97** (2006), 216102.
87) Y. Shibuta, K. Oguchi and T. Suzuki: *ISIJ Int.*, **52** (2012), 2205.
88) Y. Watanabe, Y. Shibuta and T. Suzuki: *ISIJ Int.*, **50** (2010), 1158.
89) J. Monk, Y. Yang, M. I. Mendelev, M. Asta, J. J. Hoyt and D. Y. Sun: *Modell. Simul. Mater. Sci. Eng.*, **18** (2010), 015004.
90) M. I. Mendelev, M. J. Rahman, J. J. Hoyt and M. Asta: *Modell. Simul. Mater. Sci. Eng.*, **18** (2010), 074002.
91) Y. F. Gao, Y. Yang, D. Y. Sun, M. Asta and J. J. Hoyt: *J. Cryst. Growth*, **312** (2010), 3238.
92) D. Buta, M. Asta and J. J. Hoyt: *J. Chem. Phys.*, **127** (2007), 074703.
93) J. J. Hoyt, A. Karma, M. Asta and D. Y. Sun: *JOM*, **56** (2004), 49.
94) J. Bragard, A. Karma, Y. H. Lee and M. Plapp: *Interface Sci.*, **10** (2002), 121.
95) T. Haxhimali, A. Karma, F. Gonzales and M. Rappaz: *Nature Mater.*, **5** (2006), 660.
96) H. Kasajima, E. Nagano, T. Suzuki, S. Gyoon Kim and W. Tae Kim: *Sci. Technol. Adv. Mater.*, **4** (2003), 553.
97) K. Kuniyoshi, K. Ozono, M. Ikeda, T. Suzuki, S. Gyoon Kim and W. Tae Kim: *Sci. Technol. Adv. Mater.*, **7** (2006), 595.
98) T. Suzuki, S. G. Kim and W. T. Kim: *Mater. Sci. Eng. A*, **449–451** (2007), 99.
99) S. G. Kim and W. T. Kim: *J. Cryst. Growth*, **275** (2005), e355.
100) L. Gránásy, T. Pusztai and J. A. Warren: *J. Phys.: Condens. Matter*,

16 (2004), R1205.
101) L. Gránásy, T. Pusztai, G. Tegze, J. A. Warren and J. F. Douglas: *Phys. Rev. E*, **72** (2005), 011605.
102) J. J. Eggleston, G. B. McFadden and P. W. Voorhees: *Physica D*, **150** (2001), 91.
103) S. Torabi, J. Lowengrub, A. Voigt and S. Wise: *Proc. of the Royal Society A: Math. Phys. Eng. Sci.*, **465** (2009), 1337.
104) S. Wise, J. Kim and J. Lowengrub: *J. Comput. Phys.*, **226** (2007), 414.
105) A. A. Wheeler: *Proc. of the Royal Society A: Math. Phys. Eng. Sci.*, **462** (2006), 3363.
106) H. K. Lin, C. C. Chen and C. W. Lan: *J. Cryst. Growth*, **362** (2013), 62.
107) J. Friedli, P. Di Napoli, M. Rappaz and J. A. Dantzig: *IOP Conf. Ser.: Mater. Sci. Eng.*, **33** (2012), 012111.
108) J.-M. Debierre, A. Karma, F. Celestini and R. Guérin: *Phys. Rev. E*, **68** (2003), 041604.
109) R. Guérin, J.-M. Debierre and K. Kassner: *Phys. Rev. E*, **71** (2005), 011603.
110) T. Uehara and R. F. Sekerka: *J. Cryst. Growth*, **254** (2003), 251.
111) H. Miura: *J. Cryst. Growth*, **367** (2013), 8.
112) M. Chen, X.-D. Hu, D.-Y. Ju and H.-Y. Zhao: *Comput. Mater. Sci.*, **79** (2013), 684.
113) S. Gurevich, M. Amoorezaei, D. Montiel and N. Provatas: *Acta Mater.*, **60** (2012), 3287.
114) M. Amoorezaei, S. Gurevich and N. Provatas: *Acta Mater.*, **60** (2012), 657.
115) M. Wang, T. Jing and B. Liu: *Scr. Mater.*, **61** (2009), 777.
116) M. Y. Wang, J. J. Williams, L. Jiang, F. De Carlo, T. Jing and N. Chawla: *Scr. Mater.*, **65** (2011), 855.
117) I. Steinbach, F. Pezzolla, B. Nestler, M. Seeßelberg, R. Prieler, G. J. Schmitz and J. L. L. Rezende: *Physica D*, **94** (1996), 135.
118) J. Tiaden, B. Nestler, H. J. Diepers and I. Steinbach: *Physica D*, **115** (1998), 73.
119) I. Steinbach and F. Pezzolla: *Physica D*, **134** (1999), 385.
120) J. Eiken, B. Böttger and I. Steinbach: *Phys. Rev. E*, **73** (2006), 066122.
121) B. Böttger, J. Eiken and I. Steinbach: *Acta Mater.*, **54** (2006), 2697.
122) I. Steinbach, B. Böttger, J. Eiken, N. Warnken and S. G. Fries: *J. Phase Equilib. Diff.*, **28** (2007), 101.
123) S. G. Kim, W. T. Kim, T. Suzuki and M. Ode: *J. Cryst. Growth*, **261** (2004), 135.
124) S. G. Kim: *Acta Mater.*, **55** (2007), 4391.
125) B. Nestler, H. Garcke and B. Stinner: *Phys. Rev. E*, **71** (2005), 041609.
126) B. Nestler and A. A. Wheeler: *Phys. Rev. E*, **57** (1998), 2602.
127) B. Nestler and A. A. Wheeler: *Comput. Phys. Commun.*, **147** (2002), 230.
128) A. Carré, B. Böttger and M. Apel: *J. Cryst. Growth*, **380** (2013), 5.
129) A. Choudhury and B. Nestler: *Phys. Rev. E*, **85** (2012), 021602.
130) R. Kobayashi, J. A. Warren and W. C. Carter: *Physica D*, **119** (1998), 415.
131) J. A. Warren, W. C. Carter and R. Kobayashi: *Physica A*, **261** (1998), 159.
132) R. Kobayashi and Y. Giga: *J. Stat. Phys.*, **95** (1999), 1187.
133) J. A. Warren, R. Kobayashi and W. Craig Carter: *J. Cryst. Growth*, **211** (2000), 18.
134) R. Kobayashi, J. A. Warren and W. C. Carter: *Physica D*, **140** (2000), 141.
135) J. A. Warren, R. Kobayashi, A. E. Lobkovsky and W. C. Carter: *Acta Mater.*, **51** (2003), 6035.
136) L. Gránásy, T. Pusztai, T. Börzsönyi, J. A. Warren and J. F. Douglas: *Nat. Mater.*, **3** (2004), 645.
137) L. Granasy, T. Pusztai, J. A. Warren, J. F. Douglas, T. Borzsonyi and V. Ferreiro: *Nat. Mater.*, **2** (2003), 92.
138) D. M. Anderson, G. B. McFadden and A. A. Wheeler: *Annu. Rev. Fluid Mech.*, **30** (1998), 139.
139) D. M. Anderson, G. B. McFadden and A. A. Wheeler: *Physica D*, **135** (2000), 175.
140) G. B. McFadden, A. A. Wheeler and D. M. Anderson: *Physica D*, **144** (2000), 154.
141) D. M. Anderson, G. B. McFadden and A. A. Wheeler: *Physica D*, **151** (2001), 305.
142) R. Tönhardt and G. Amberg: *J. Cryst. Growth*, **194** (1998), 406.
143) R. Tönhardt and G. Amberg: *J. Cryst. Growth*, **213** (2000), 161.
144) R. Tönhardt and G. Amberg: *Phys. Rev. E*, **62** (2000), 828.
145) C. Beckermann, H.-J. Diepers, I. Steinbach, A. Karma and X. Tong: *J. Comput. Phys.*, **154** (1999), 468.
146) H.-J. Diepers, C. Beckermann and I. Steinbach: *Acta Mater.*, **47** (1999), 3663.
147) X. Tong, C. Beckermann and A. Karma: *Phys. Rev. E*, **61** (2000), R49.
148) X. Tong, C. Beckermann, A. Karma and Q. Li: *Phys. Rev. E*, **63** (2001), 061601/1.
149) C. Lan and C. Shih: *Phys. Rev. E*, **69** (2004), 031601.
150) C. W. Lan, C. M. Hsu and C. C. Liu: *J. Cryst. Growth*, **241** (2002), 379.
151) C. W. Lan, C. M. Hsu, C. C. Liu and Y. C. Chang: *Phys. Rev. E*, **65** (2002), 061601/1.
152) W. Miller, I. Rasin and F. Pimentel: *J. Cryst. Growth*, **266** (2004), 283.
153) D. Medvedev, T. Fischaleck and K. Kassner: *Phys. Rev. E*, **74** (2006), 031606.
154) D. Medvedev, T. Fischaleck and K. Kassner: *J. Cryst. Growth*, **303** (2007), 69.
155) D. Medvedev and K. Kassner: *Phys. Rev. E*, **72** (2005), 056703.
156) D. Medvedev and K. Kassner: *J. Cryst. Growth*, **275** (2005), e1495.
157) M. Selzer, M. Jainta and B. Nestler: *Phica Satus Slidi (b)*, **246** (2009), 1197.
158) Z. Guo, J. Mi and P. S. Grant: *IOP Conf. Ser.: Mater. Sci. Eng.*, **33** (2012), 012101.
159) Z. Guo, J. Mi, S. Xiong and P. S. Grant: *Metall. Mater. Trans. B*, **44** (2013), 924.
160) R. S. Qin and E. R. Wallach: *Mater. Sci. Eng. A*, **357** (2003), 45.
161) Y. Natsume, K. Ohsasa and T. Narita: *Mater. Trans.*, **43** (2002), No. 9, 2228.
162) R. Siquieri, J. Rezende, J. Kundin and H. Emmerich: *Eur. Phys. J. Spec. Top.*, **177** (2009), 193.
163) H. Neumann-Heyme, K. Eckert and S. Odenbach: *IOP Conf. Ser.: Mater. Sci. Eng.*, **27** (2012), 012045.
164) Y. Sun and C. Beckermann: *J. Cryst. Growth*, **311** (2009), 4447.
165) B. Nestler, A. A. Wheeler, L. Ratke and C. Stöcker: *Physica D*, **141** (2000), 133.
166) J.-H. Jeong, N. Goldenfeld and J. Dantzig: *Phys. Rev. E*, **64** (2001), 416021.
167) J.-H. Jeong, J. A. Dantzig and N. Goldenfeld: *Metall. Mater. Trans. A*, **34** (2003), 459.
168) Y. Lu, C. Beckermann and J. C. Ramirez: *J. Cryst. Growth*, **280** (2005), 320.
169) C. C. Chen and C. W. Lan: *J. Cryst. Growth*, **312** (2010), 1437.
170) C. C. Chen, Y. L. Tsai and C. W. Lan: *Int. J. Heat Mass Transfer*, **52** (2009), 1158.
171) J. Rosam, P. K. Jimack and A. M. Mullis: *Acta Mater.*, **56** (2008), 4559.
172) J. Narski and M. Picasso: *Comput. Meth. Appl. Mech. Eng.*, **196** (2007), 3562.
173) T. Takaki, T. Fukuoka and Y. Tomita: *J. Cryst. Growth*, **283** (2005), 263.
174) C. W. Lan and Y. C. Chang: *J. Cryst. Growth*, **250** (2003), 525.
175) C. W. Lan, Y. C. Chang and C. J. Shih: *Acta Mater.*, **51** (2003), 1857.
176) R. J. Braun and B. T. Murray: *J. Cryst. Growth*, **174** (1997), 41.
177) N. Provatas, N. Goldenfeld and J. Dantzig: *J. Comput. Phys.*, **148** (1999), 265.
178) N. Provatas, N. Goldenfeld and J. Dantzig: *Phys. Rev. Lett.*, **80** (1998), 3308.
179) C. C. Chen and C. W. Lan: *J. Cryst. Growth*, **311** (2009), 702.
180) K. Oguchi and T. Suzuki: *Mater. Trans.*, **48** (2007), 2280.
181) K. Oguchi and T. Suzuki: *ISIJ Int.*, **47** (2007), 277.
182) D. Danilov and B. Nestler: *J. Cryst. Growth*, **275** (2005), e177.
183) H. M. Singer, I. Singer-Loginova, J. H. Bilgram and G. Amberg: *J. Cryst. Growth*, **296** (2006), 58.
184) Y. B. Altundas and G. Caginalp: *Nonlinear Anal.: Theo.*, **62** (2005), 467.
185) Z. Guo, J. Mi and P. S. Grant: *J. Comput. Phys.*, **231** (2012), 1781.
186) W. L. George and J. A. Warren: *J. Comput. Phys.*, **177** (2002), 264.
187) J. Eiken: *Int. J. Cast Metal. Res.*, **22** (2009), 86.
188) I. Steinbach: *Acta Mater.*, **56** (2008), 4965.
189) K. Kassner, R. Guérin, T. Ducousso and J.-M. Debierre: *Phys. Rev. E*, **82** (2010), 021606.
190) S. Gurevich, A. Karma, M. Plapp and R. Trivedi: *Phys. Rev. E*, **81** (2010), 011603.
191) N. Bergeon, D. Tourret, L. Chen, J. M. Debierre, R. Guérin, A. Ramirez, B. Billia, A. Karma and R. Trivedi: *Phys. Rev. Lett.*, **110** (2013), 226102.
192) N. Bergeon, R. Trivedi, B. Billia, B. Echebarria, A. Karma, S. Liu, C. Weiss and N. Mangelinck: *Adv. Space Res.*, **36** (2005), 80.
193) A. Yamanaka, T. Aoki, S. Ogawa and T. Takaki: *J. Cryst. Growth*, **318** (2011), 40.
194) L. K. Aagesen, J. L. Fife, E. M. Lauridsen and P. W. Voorhees: *Scr. Mater.*, **64** (2011), 394.
195) P. K. Galenko, S. Reutzel, D. M. Herlach, S. G. Fries, I. Steinbach and M. Apel: *Acta Mater.*, **57** (2009), 6166.
196) C. Corbella, B. Echebarria, L. Ramírez-Piscina, E. Pascual, J. L. Andújar and E. Bertran: *Acta Mater.*, **57** (2009), 4948.
197) P. K. Galenko, S. Reutzel, D. M. Herlach, D. Danilov and B. Nestler: *Acta Mater.*, **55** (2007), 6834.
198) M. Amoorezaei, S. Gurevich and N. Provatas: *Acta Mater.*, **58** (2010), 6115.
199) Y. Chen, A. A. Bogno, N. M. Xiao, B. Billia, X. H. Kang, H. Nguyen-Thi, X. H. Luo and D. Z. Li: *Acta Mater.*, **60** (2012), 199.
200) Y. Chen, A. A. Bogno, B. Billia, X. H. Kang, H. Nguyen-Thi, D. Z. Li, X. H. Luo and J. M. Debierre: *ISIJ Int.*, **50** (2010), 1895.